

## Spatial retarding field energy analyzer measurements downstream of a helicon double layer plasma

W. Cox,<sup>1,a)</sup> C. Charles,<sup>1</sup> R. W. Boswell,<sup>1</sup> and R. Hawkins<sup>2</sup>

<sup>1</sup>Space Plasma, Power, and Propulsion Group, Research School of Physical Sciences and Engineering, The Australian National University, Australian Capital Territory 0200, Australia

<sup>2</sup>Vizlab, ANU Supercomputing Facility, The Australian National University, Australian Capital Territory 0200, Australia

(Received 2 June 2008; accepted 7 July 2008; published online 20 August 2008)

Spatial ion energy measurements using a retarding field energy analyzer are performed in the exhaust of a 0.30 mTorr, 250 W helicon double layer plasma to investigate the divergence of the argon ion beam formed by acceleration in the double layer. Various divergence angles are computed by considering the radial distribution of beam density; the average beam ion diverging by  $9^\circ$ . The efficiency at which momentum is imparted parallel to the longitudinal axis of the thruster is calculated to be 98%. The results show that a few centimeters downstream of the source, the beam ions do not follow the magnetic field lines. © 2008 American Institute of Physics.

[DOI: 10.1063/1.2965866]

Recent experimental,<sup>1-3</sup> analytical,<sup>4-6</sup> and simulation<sup>7</sup> studies on ion beams accelerated by electric double layers spontaneously formed in expanding magnetized plasmas have attracted great interest in the field of space science<sup>8</sup> and plasma propulsion.<sup>9</sup> A new type of plasma thruster, the helicon double layer thruster (HDLT), has been recently developed and tested for a variety of gases.<sup>10-12</sup> Electric propulsion of spacecraft is employed when a small thrust with a high specific impulse is appropriate to the mission profile: e.g., station keeping and long range interplanetary trajectories. One source of fuel and energy inefficiency in rocket propulsion is divergence of the exhaust plume. Computer simulations of the trajectories of ions accelerated by the HDLT suggest that the exhaust plasma beam would diverge very little.<sup>13,14</sup> However, the simulations were single particle without Poisson's equation and did not take into account any plasma phenomena. In this letter the first experimental two dimensional spatial characterization of the ion beam in the helicon double layer plasma experiment is carried out using an energy analyzer to verify the earlier simulations.

The Chi Kung plasma source,<sup>15</sup> identical to the HDLT, is attached contiguously to the diffusion chamber in which the ion beam is detected. The interface between the 31 cm long, 13.7 cm internal diameter Pyrex source tube and the 29.5 cm long, 32 cm diameter Al expansion chamber is defined as  $z=30$  cm, as detailed previously<sup>15</sup> and shown in Fig. 1. Here the double saddle antenna surrounding the source tube has been flipped horizontally and rotated  $90^\circ$ , compared to the orientation used in Ref. 15. The antenna is supplied with 250 W of rf power via a  $\pi$ -matching network. Surrounding the source tube, the two solenoids provide a magnetic field of  $\sim 140$  G in the source ( $z=21$  cm) and a few tens of gauss in the diffusion chamber.<sup>16</sup> A base pressure of a few microtorrs is provided by a turbomolecular/primary pump system connected to the vacuum chamber. Argon is injected via another chamber sideport and a constant pressure of 0.30 mTorr measured on a baratron gauge is presently maintained.

A spatial investigation of the ion beam properties is performed by sweeping a retarding field energy analyzer<sup>17</sup> (RFEA) across the source tube exit with its aperture hole facing the plasma source. The RFEA support tube comprises two  $90^\circ$  bends (commonly called a DogLeg) facilitating a circular rotation by offsetting the RFEA orifice 107 mm from the fulcrum (Fig. 1). Cylindrical symmetry is assumed<sup>18</sup> and a simple calculation allows the radial distance from the  $z$  axis corresponding to each probe rotation to be determined. Mapping the two dimensional region from  $z=31$  cm to  $z=44.5$  cm,  $r=0$  cm to  $r=13.7$  cm is achieved by performing ten circular sweeps in 1.5 cm axial intervals. Assuming azimuthal symmetry, this region can be doubled by mirroring the  $r=0$  cm to  $r=13.7$  cm region such that the downstream region from wall to wall is mapped in the region  $z=31$  cm to  $z=44.5$  cm.

The collector current versus discriminator voltage RFEA characteristic  $I_c(V_d)$  is spatially measured in the exhaust of the helicon double layer plasma and the first derivative, called the ion energy distribution function (IEDF), is fitted by analytical Gaussian functions using a previously described deconvolution method.<sup>15</sup> Each IEDF is represented by the sum of a low and a high energy Gaussian which

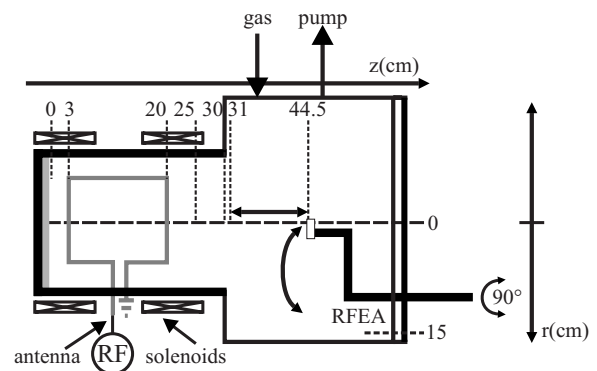


FIG. 1. Schematic of the Chi Kung reactor showing the helicon double layer plasma source and the diffusion chamber with diagnostic (DogLeg RFEA). Inserted through the backplate, the DogLeg RFEA is rotated through  $90^\circ$  in  $5^\circ$  intervals.

<sup>a)</sup>Electronic mail: wes.cox@anu.edu.au.

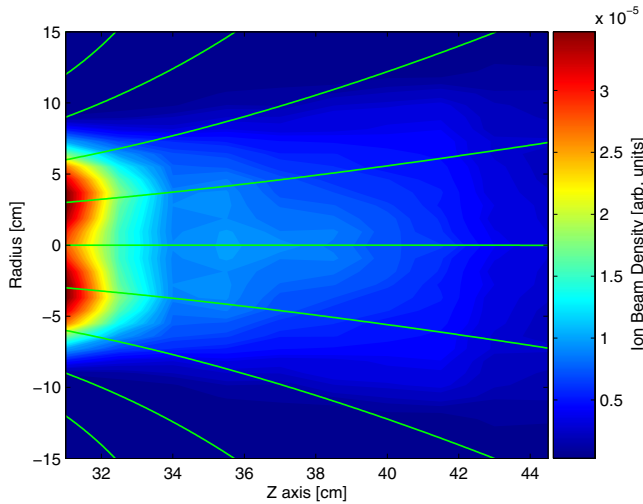


FIG. 2. (Color online) Contour plot of the ion beam density measured with the RFEA at the beam potential ( $53 \pm 1$  V). The magnetic field lines are obtained from simulation which agrees with experimental measurements.<sup>9</sup> The operating conditions are 250 W rf power, 0.30 mTorr argon pressure and a magnetic field diverging from  $\sim 140$  G at  $z=21$  cm to  $\sim 10$  G at  $z=45$  cm.<sup>16</sup> The vertical axis is plotted from  $-15$  to  $+15$  cm, the negative radius has been artificially introduced to indicate opposite sides of the reactor  $z$  axis.

correspond to the two ion energy populations present in the downstream plasma: the local plasma ions and the higher energy beam ions, respectively. The energy difference between these two ion energy populations, under these experimental conditions, is found to be  $\sim 15$  V, where the beam ions are found to have a consistent energy of  $eV_b = 53 \pm 1$  eV over the range  $z=31$ – $44.5$  cm. This value corresponds to the plasma potential measured just upstream of the double layer.<sup>16</sup> Hence the beam density can be directly obtained from the beam flux  $n_b \propto I_c/V_b$ , where  $n_b$  is the beam density and  $I_c$  is the collector current.<sup>10</sup> Figures 2 and 3 show the two dimensional contour and cross sections for a selection of RFEA sweeps of beam ion density, respectively. In the exhaust area ( $z > 34$  cm) the beam decays exponentially with a decay constant  $\lambda \sim 13$  cm, close to the ion-neutral mean free path for charge exchange.<sup>4</sup> The calculation of the

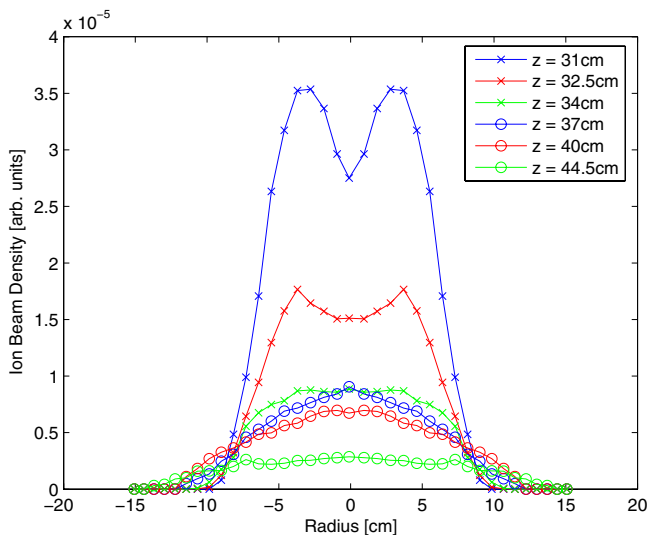


FIG. 3. (Color online) The beam ion density profile for various axial  $z$  positions. Similar to Fig. 2, the radial axis contains artificial negative values.

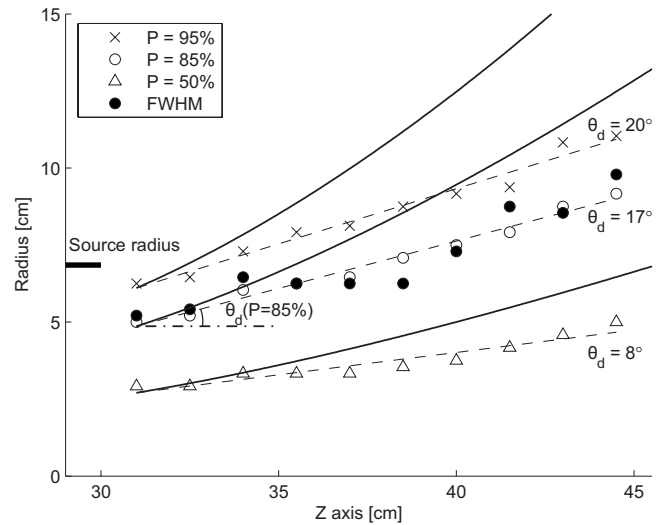


FIG. 4. Divergence angles  $\theta_d(P)$  calculated from the integration percentages  $P=50\%$ ,  $85\%$ , and  $95\%$  of each  $z$  slice. The magnetic field lines that pass through the beam edge best-fit point at  $z=31$  cm are shown as solid lines. The divergence angle  $\theta_d$ , measured from the reactor  $z$  axis to each integrated beam edge, is shown for an integrated percentage of  $85\%$ .

magnetic field in the reactor generates the curved field lines overlaid in Fig. 2 and shows no correlation between the divergence of the ion beam and the divergent magnetic field. Just downstream of the source exit ( $z=31$  cm) the profile has a double-hump form which becomes a single peak within 3 cm (Fig. 3). The double-hump profile is indicative of an inductively coupled plasma in the source.<sup>10</sup> It is difficult to determine a value for the divergence of the ion beam. There are various color interfaces in Fig. 2 indicating density gradients, however, there are no regions showing a distinct edge. For each  $z$  slice, integration of the beam ion density out from the center ( $r=0$  cm) until an integration percentage  $P$  of the total density is reached defines an edge to the beam,

$$P = 100 \times \frac{\int_{r=0}^{r=R} n(r) dr}{\int_{r=0}^{r=\text{wall}} n(r) dr}, \quad (1)$$

where  $r$  is the radius,  $n(r)$  is the ion density,  $P$  is the integration percentage, and  $R$  is the beam edge radius for this percentage in this slice. Figure 4 shows some beam edges and lines of best fit measuring the divergence angles for various integration percentages  $P$ , including the calculated full width half maximum (FWHM) point for each  $z$  slice. The exhaust plume FWHM from Chi Kung is shown to lie essentially on the beam edge for an  $85\%$  density integration, indicating a tight confinement of the plume about the  $z$  axis of the reactor. A divergence angle  $\theta_d$ , defined as the angle between the reactor  $z$  axis and the beam edge line of best fit, can be obtained for each value of  $P$ .  $\theta_d$  is found to be  $8^\circ$ ,  $17^\circ$ , and  $20^\circ$  for integrated percentages  $P=50\%$ ,  $85\%$ , and  $95\%$ , respectively. The independence of the magnetic field lines and the beam edge (under various definitions) is confirmed by comparing the magnetic field lines and the beam edges at  $z=31$  cm in Fig. 4. It can be seen that the magnetic field lines curve away, with the angle increasing as a function of  $z$ , while the beam edge remains approximately linear.

Determination of the beam divergence under various criteria enables calculation of the efficiency at which momentum is transferred to the thruster by the propulsion of ions accelerated in the double layer. An ion propelled at an angle

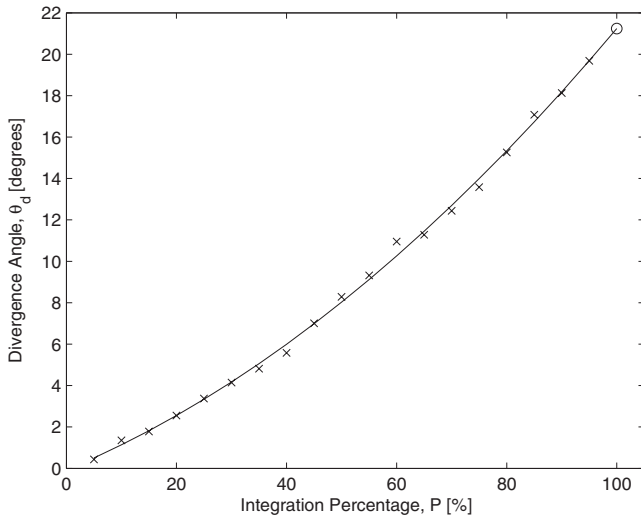


FIG. 5. The crosses show the divergence angles  $\theta_d$  as a function of integrated percentage  $P$ . The solid line is the quadratic line of best fit. The inferred 100% point is plotted as the circle.

to the  $z$  axis transfers momentum to the thruster, reduced by the cosine of the angle. If the radial motion of the accelerated ions is the result of a cylindrically symmetric phenomenon (such as a spherically curved double layer<sup>19</sup>), then the radial momentum components cancel out resulting in the net (reduced) momentum in the desired direction. It is the ratio between this net momentum to the total ejected ion momentum that is of interest in this study of beam divergence as it provides a means of evaluating a source of thruster inefficiency. The momentum efficiency  $\epsilon_{\text{mom}}$  is calculated by

$$\epsilon_{\text{mom}} = 100 \times \sum_{P=5\%}^{100\%} 0.05 \cos \theta_d(P), \quad (2)$$

where  $\theta_d(P)$  is the angle of divergence as a function of the integration percentage  $P$ , Eq. (1). Computation of the momentum efficiency is obtained by decomposing the beam density into 5% integration steps from the center to obtain various values for  $R$  in Eq. (1). With these values of  $R$  for each  $z$  slice, the associated divergence angles for each integration percentage can be determined. Summing the cosines of these angles appropriately scaled by the integration step (5%) thus produces the momentum efficiency  $\epsilon_{\text{mom}}$ . Figure 5 shows the behavior of the divergence angle  $\theta_d$  as a function of integration percentage  $P$ . The 100% point is inferred from the quadratic fit to the other points. The divergence in the center of the beam is seen to be very low ( $<0.5^\circ$ ) and in-

creases quadratically with the integrated beam density percentage. Thus if we were to choose a divergence criterion of some integration percentage and use it to quote the divergence of the beam, it would be incorrect to assume that all the particles are ejected from the source at this angle. Indeed the majority of the beam would be emitted at an angle lower than the quoted value. This effect is manifested in the high momentum efficiency. From Eq. (2) the momentum efficiency is  $\epsilon_{\text{mom}}=98\%$  for the Chi Kung reactor under the conditions described above. This implies that for all the momentum imparted to the ions in the various directions, 98% of that momentum is parallel to the  $z$  axis and potentially provides thrust.

In summary, investigation into the two dimensional spatial properties of the downstream ion density at the beam potential produces an estimation of the beam divergence downstream of a helicon double layer plasma. The divergence angle is found to increase as a greater percentage of the beam density is considered with an average divergence of  $9^\circ$ . More importantly, the centrally dense beam distribution results in a momentum efficiency of 98%.

- <sup>1</sup>C. Charles and R. W. Boswell, *Appl. Phys. Lett.* **82**, 1356 (2003).
- <sup>2</sup>S. A. Cohen, N. S. Siefert, S. Stange, R. F. Boivin, E. E. Scime, and F. M. Levinton, *Phys. Plasmas* **10**, 2593 (2003).
- <sup>3</sup>X. Sun, A. M. Keesee, C. Biloiu, E. E. Scime, A. Meige, C. Charles, and R. W. Boswell, *Phys. Rev. Lett.* **95**, 025004 (2005).
- <sup>4</sup>M. A. Lieberman and C. Charles, *Phys. Rev. Lett.* **97**, 045003 (2006).
- <sup>5</sup>A. Fruchtman, *Phys. Rev. Lett.* **96**, 065002 (2006).
- <sup>6</sup>F. F. Chen, *Phys. Plasmas* **13**, 034502 (2006).
- <sup>7</sup>A. Meige, R. W. Boswell, C. Charles, and M. M. Turner, *Phys. Plasmas* **12**, 052317 (2005).
- <sup>8</sup>R. W. Boswell, E. Marsch, and C. Charles, *Astrophys. J.* **640**, L199 (2006).
- <sup>9</sup>C. Charles, *Plasma Sources Sci. Technol.* **16**, R1 (2007).
- <sup>10</sup>C. Charles, R. W. Boswell, and M. A. Lieberman, *Appl. Phys. Lett.* **89**, 261503 (2006).
- <sup>11</sup>M. D. West, C. Charles, and R. W. Boswell, *J. Propul. Power* **24**, 134 (2008).
- <sup>12</sup>C. Charles, R. W. Boswell, P. Alexander, C. Costa, O. Sutherland, L. Pfitzner, R. Franzen, J. Kingwell, A. Parfitt, P. E. Frigot, J. Gonzalez Del Amo, and G. Saccoccia, *IEEE Trans. Plasma Sci.* (to be published).
- <sup>13</sup>F. N. Gesto, B. D. Blackwell, C. Charles, and R. W. Boswell, *J. Propul. Power* **22**, 24 (2006).
- <sup>14</sup>F. N. Gesto, C. Charles, and R. W. Boswell, *IEEE Trans. Plasma Sci.* (to be published).
- <sup>15</sup>C. Charles and R. W. Boswell, *Phys. Plasmas* **11**, 1706 (2004).
- <sup>16</sup>C. Charles and R. W. Boswell, *Appl. Phys. Lett.* **91**, 201505 (2007).
- <sup>17</sup>C. Charles, A. W. Degeling, T. E. Sheridan, J. H. Harris, M. A. Lieberman, and R. W. Boswell, *Phys. Plasmas* **7**, 5232 (2000).
- <sup>18</sup>W. Cox, R. Hawkins, C. Charles, and R. W. Boswell, *IEEE Trans. Plasma Sci.* (to be published).
- <sup>19</sup>N. Plihon, P. Chabert, and C. S. Corr, *Phys. Plasmas* **14**, 013506 (2007).